Tracing groundwater recharge sources in a mountain-plain transitional area using stable isotopes and hydrochemistry

Yaping Liu[a,*], Tsutomu Yamanaka[b]

[a] Graduate School of Life and Environmental Sciences, University of Tsukuba, Japan

[b] Terrestrial Environment Research Center, University of Tsukuba, Japan

[*] Corresponding author. Yaping Liu, Graduate School of Life and Environmental Sciences, University of Tsukuba, Tsukuba, Ibaraki 305-8577, Japan. E-mail: liulydia1010@gmail.com (Y. Liu); tyam@suiri.tsukuba.ac.jp (T. Yamanaka).

Abstract

Mountain-plain transitional landscapes are especially important as groundwater recharge zones. In this study, the oxygen and hydrogen stable isotopic composition ($\delta^{18}O$ and δD) of water and hydrochemical information were employed to quantify contribution ratios of different sources of groundwater recharge in the Ashikaga area of central Japan. The study area is situated between the Ashio Mountains and the Kanto plain, and the Watarase River flows into the region parallel to the mountain-plain boundary. There was an obvious isotopic altitude effect in and around the study area (-0.25‰ per 100 m for $\delta^{18}O$ and -1.7‰ per 100 m for δD), and the isotopic signatures of water from the Watarase River and local precipitation could be clearly distinguished. In addition, it was possible to identify the occurrence of mountain block recharge using hydrochemistry, specifically the chloride ion. End-member mixing analysis using δ values and Cl^- concentration revealed spatial variation in the contribution ratios of the river water, mountain block groundwater and local precipitation. Seepage from the Watarase River contributed a significant amount of water to aquifers along its channel. The river-recharged water reached 5 km from the channel in the south (i.e., plain) side and 1.6 km or less in the north (i.e., mountain) side. Remarkable mountain block recharge was observed in the foothills near the axis of the syncline, which has layers of chert and sandstone that likely hinder river channel seepage into the mountain-side aquifers. Major factors controlling the river-water contribution ratio include the distance from the river channel, topography, and hydrogeological settings. The results presented here should facilitate integrated management of groundwater and surface water resources.

Key words: Groundwater recharge, river channel seepage, mountain block recharge, end-member mixing analysis (EMMA), isotopic tracer, groundwater-river interaction

1. Introduction

A large amount of groundwater recharge occurs along mountain fronts in semiarid regions (Wilson and Guan, 2004). Even under humid climates, deep groundwater in plains aquifers is recharged along the margins of plains adjacent to mountains (Mikita et al., 2011; Yamanaka et al., 2011a). Clearly identifying recharge sources and their corresponding contributions is prerequisite to sustainable management of aquifers to ensure that the needs of humans and ecosystems are met. Groundwater recharge in mountain-plain transitional areas can generally be divided into direct recharge of local precipitation and mountain-front recharge. Mountain-front recharge is subdivided into surface and subsurface components, with the former representing seepage from surface water bodies (e.g., river seepage) and the latter consisting of mountain block recharge, which is the subsurface water flow from the mountain block to an adjacent basin (Manning and Solomon, 2005; Aishlin and McNamara, 2011).

Numerous studies have demonstrated that river water seepage is an important recharge mechanism along river reaches (Vanderzalm et al., 2011). So-called “induced flow” from rivers can occur to replenish water levels in aquifers that have been depleted as a result of groundwater abstraction (Sanz et al., 2011). However, overexploitation of water resources in the upstream and midstream portions of a river can cause groundwater decline and quality deterioration in downstream regions (Xi et al., 2010). In addition, mountain block recharge can be restricted by geological structures such as faults and folds (Wilson and Guan, 2004). For example, a normal fault can act as a conduit for the transfer of precipitation in mountain areas to a plain (Yuan et al. 2011). Geological folding diverts groundwater along syncline axes from mountain aquifers toward rift valley aquifers (Laronne Ben-Itzhak and Gvirtzman, 2005).

The hydrochemistry and isotope tracer approaches have been widely used for determination of recharge fluxes based on conceptually simple models (de Vries and Simmers, 2002). Stable isotopic compositions of groundwater recharged through direct infiltration of precipitation will reflect that of local precipitation (Clark and Fritz, 1997). If rivers retain the depleted isotopic signature of their headwaters, the difference in stable isotope signatures of rivers and local precipitation can be used to determine the relative contribution of these two sources of groundwater recharge (Scanlon et al., 2002; Lambs, 2004; Kalbus et al., 2006). Hydrochemical data can be used to complement isotopic information. Such an approach is especially useful in areas for which hydrometric data are not available.

We present here a case study of groundwater recharge and groundwater-river interaction in a mountain-plain transitional area with syncline geological settings. The specific objectives of the present study are to identify recharge sources of groundwater and quantitatively evaluate their contribution ratio using stable isotopes and hydrochemistry, with a special emphasis on the spatial extent of river-recharged groundwater and its controlling factors.

2. Material and methods

2.1. Study area

The Ashikaga area of central Japan (Fig. 1) was selected as the study site. This area is situated at the northern margin of the Kanto Plain, which is the largest plain in Japan. The area is bounded on the north by the Ashio Mountains. The Watarase River, which has a total length of 106.7 km, originates in Mt. Sukai (elevation, 2,144 m above mean sea level (a.m.s.l.)) in the Ashio Mountains (Fig. 1a) and runs across the central part of the study area. The river flows to the southwest and then turns southeast along the margin of the plain. The study area is located in the middle reaches of this river (Fig. 1b). There are several tributaries to the Watarase within the study area that originate in low mountains with elevations that range from 223 to 681 m a.m.s.l. Since the discharge rates of tributaries are far less than the Watarase River and all the river banks are built using pebble and concrete, the river seepage of tributaries was neglected and the Watarase River seepage was the focus in this study.

The study area is located in a humid temperate zone that shows broad variations in temperature. Summer in the region is characterized by warm and humid conditions, while winter is cold and relatively arid. Based on observed data collected by the Japan

Meteorological Agency (http://www.jma.go.jp/jma/index.html) from 1981-2010, the monthly mean air temperature ranges from 2.8 ℃ (January) to 25.7 ℃ (August), and the annual precipitation is approximately 1,200 mm. About 75% of the annual precipitation occurs during the rainy season from May to October. The precipitation data were collected from Ashikaga Station (36°18.1' N, 139°28.4' E and 28 m a.m.s.l.), while the temperature data were from Sano Station (36°21.8' N, 139°34.2'E and 68 m a.m.s.l.).

Forest is the dominant land cover for the mountains, while residential areas are mainly located in the lowlands along the Watarase River. Rice paddy fields are also distributed along the Watarase River and its tributaries, but their total area accounts for only 10% of the entire study area and most of them are far from the sampled wells. In addition, irrigation occurs during rainy seasons from June to September. Therefore, seepage from paddy fields is expected to be a minor recharge source for most of the sites in our study area.

No facilities consuming large amounts of water were found in the study area, except for seven water purification plants (AT1 - AT7 in Fig. 1) with 17 municipal wells. These plants are distributed along the Watarase River and supply tap water to local residents. The municipal water supply system in Ashikaga City is solely dependent on groundwater. In addition to tap water, many residents also utilize water drawn from private wells on their own land for domestic purposes. Because these wells are private, hydrometric measurements are not available. However, the well depths of some wells were inquired from local owners and most of the wells are shallow wells with depth between 5-12 m except one deep well (AW6 in Fig. 1), of which depth is 150 m. In addition, the municipal wells of AT1, AT2, AT3 and AT5 are also shallow wells with depth no more than 11 m. Although municipal wells AT4, AT6 and AT7 are deep wells with depth 40-80 m, their well screens are multi-depths and the uppermost screens are in the shallow aquifer. It should also be noted that the drainage system in the study area is well developed; therefore, domestic wastewater can be rapidly drained to rivers and away from the study area without re-entering local groundwater systems. Accordingly, the seepage of domestic wastewater to groundwater in the study area was not considered in this study.

2.2. Geographical and hydrogeological settings

As shown on the surficial geology map (Fig. 2a), the mountains in the study area are characterized by a series of distinct NE-SW trending anticline and syncline tectonic movements. The lithology of the mountains consists mostly of chert, sandstone with interbedded slate or mudstone, and some limestone. Plains and valleys in the region are overlain by recent alluvial sediments (sand and gravel) and volcanic soil (loam). The geologic cross section (Fig. 2b) shows that the thickness of the aquifer increases from 55 to more than 150 m from northwest to southeast in the plain. The aquifer is mainly composed of gravel and sand, and the aquitard consists of red and blue clay. The bedrock is composed of chert.

2.3. Sampling and analysis

Precipitation samples were collected monthly during a 1-year period from November 2010 to October 2011. Field surveys were carried out six times approximately bimonthly during the period. Overall, 12 groundwater samples were collected from private wells (AW1-AW12 in Fig. 1) and four river water samples (AR1-AR4 in Fig.1) were collected at each sampling point. Water temperature, electrical conductivity (EC) and pH were measured in situ with portable instruments. Additionally, groundwater samples from 17 municipal wells utilized by seven water purification plants (AT1-AT7 in Fig. 1) were collected monthly from December 2010 to October 2011. All samples were subjected to isotope analysis. In addition, hydrochemical analysis was conducted using 23 groundwater samples collected from private wells and seven river water samples in September 2010 and April 2011, and 8 groundwater samples from municipal wells in September 2010.

The isotopic and chemical compositions of the water samples were analyzed at the Terrestrial Environment Research Center, University of Tsukuba. The hydrogen and oxygen stable isotopic composition of the water samples were determined using a liquid water isotope analyzer (L1102-i, Picarro, Santa Clara, CA, USA) based on wavelength-scanned cavity ring-down spectroscopy (WS-CRDS; Gupta et al., 2009). The isotopic ratios of ^{18}O and D were expressed as $\delta^{18}O$ and δD, respectively, relative to the Vienna Standard Mean Ocean Water. The analytical errors were 0.1‰ for $\delta^{18}O$ and 1‰ for δD (Yamanaka and Onda, 2011) for samples collected from November 2010 to July 2011, while they were 0.2‰ for $\delta^{18}O$ and 2‰ for δD for samples collected after August 2011 owing to replacement of the analyzer. Cation and anion concentrations were measured using an ion chromatograph (LC-10AP, Shimadzu, Tokyo, Japan) with an analytical precision of ±1 mg/L. The bicarbonate concentration was measured by the titration method using sulfuric acid. The accuracy of the hydrochemical analyses was checked using an electrical balance. Samples with relative errors greater than 5% were reanalyzed.

3. Results and discussion

3.1. Isotopic signatures

The isotopic compositions of precipitation change temporally in response to rainout history and various factors such as temperature effect and amount effect (Clark and Fritz, 1997). The d-excess of precipitation had statistically significant, negative correlation with temperature (r = -0.87, p < 0.001). A similar tendency was reported by Waseda and Nakai (1983), who stated that it was caused by seasonal shifting of the water vapor source between the Pacific and the Sea of Japan. In contrast to the high variability in δ values of precipitation, those of river water and groundwater remained nearly constant (Fig. 3). Although the d-excess of river water and groundwater showed weak variation, its phase was not in agreement with that of precipitation. These features suggest that the mean residence times of river water and groundwater are considerably long (at least > 1 year).

As expected from the seasonal changes in the d-excess of precipitation, the local meteoric water line (LMWL) which was drawn based on 1-year observed data differed remarkably between the warm period (April-September; $\delta D = 8.65\delta^{18}O+14.8$, $r^2 = 0.98$) and the cool period (October-March; $\delta D = 8.42\delta^{18}O+23.8$, $r^2 = 0.98$). The LMWL in the warm period is very similar to the global meteoric water line (GMWL; $\delta D = 8\delta^{18}O+10$; Craig, 1961), with a slightly higher slope (Fig. 4). The observed isotopic compositions of river water and groundwater (except for AW7) were plotted along the LMWL for the warm period, indicating that precipitation in the warm period is a more effective recharge source than precipitation during the cool period. The arithmetic means of $\delta^{18}O$ and δD of water from the Watarase River (AR1 in Fig. 1) were lowest among all samples collected during the study period. The weighted (based on monthly precipitation) mean $\delta^{18}O$ and δD of precipitation were -9.26‰ and -62.5‰, respectively. Total precipitation during the period was 236 mm (20%) higher than the climatic normal, in part because an extraordinary amount of rainfall occurred in May, July and September, 2011. Therefore, the 1-year observation period may be insufficient to provide a representative isotopic signature of the local precipitation. If the climatic normals (1981-2010) of monthly precipitation are used to calculate the weighted mean δ values, significantly higher values ($\delta^{18}O$ = -8.58‰ and δD = -57.4‰) are obtained. Since the extraordinary amount of rainfall should have reduced the observed δ values of precipitation, long-term mean values in this area are expected to be higher.

A close relationship existed between the mean δ values of river water and the mean elevation of the catchment corresponding to each sampling point (Fig. 5), which reflects the well-known altitude effect (Dansgaard, 1964; Clark and Fritz, 1997). Accordingly, the low δ values of the Watarase River water (AR1) are due to the high elevation of its recharge zone. The isotopic lapse rate was calculated to be -0.25‰ per 100 m for $\delta^{18}O$ and -1.7‰ per 100 m for δD. The global average isotopic lapse rate reported by Poage and Chamberlain (2001) is -0.28‰ per 100 m for $\delta^{18}O$, which is similar to the results reported here. Based on our isotopic lapse rate and the mean elevation of the entire study area, the long-term mean $\delta^{18}O$ and δD of the local precipitation are approximately -8.26‰ and -56.6‰, respectively. Although these values are higher than the observed weighted mean values for the study period, they are consistent with our expectations. Thus, we adopted these estimated values rather than those based on only 1-year observations as the isotopic signature of the local precipitation.

The arithmetic mean values of groundwater $\delta^{18}O$ and δD at each well during the study period ranged from -9.48‰ to -7.83‰ and from -65.0‰ to -55.5‰, respectively

(Table 1). With the exception of AW7, the mean δ values of groundwater were between those of Watarase River water and the estimated local precipitation values. The isotopic composition of groundwater at AW7 (with the lowest d-excess) was plotted on the right-hand side of the meteoric water lines at a distance, suggesting that it was affected by kinetic fractionation, probably due to evaporation from water or ground surfaces. The lowest $\delta^{18}O$ and δD values were found in well AT3, which is only 0.68 km from the Watarase River. The $\delta^{18}O$ and δD of groundwater on the south side of the Watarase River ranged from -9.48 to -8.45‰ and from -65.0 to -58.9‰, respectively. Conversely, the values on the north side ranged from -9.22 to -7.83‰ and from -63.0 to -55.5‰, respectively. The values were generally more negative on the south (i.e., plain) side than the north (i.e., mountain) side, which is seemingly contrary to the altitude effect. As shown in Figure 6, the Watarase River water signal decreased with distance from the Watarase River for well waters on the south side due to the dispersion and diffusion processes. However, the relationship between δ values and the distance from the Watarase River is not very obviously for well waters on the north side. Relatively high δ values were found at AT5 and AW8 near the Watarase River and relatively low δ values were found at AW9 far from the Watarase River on the north side. Since most of the groundwater samples including AT5 and AW8 were from shallow wells, the samples could represent well mixed water signals of recharge sources very well. Although the depth of AW9 is unknown, these results suggest that the Watarase River contributes a significant amount of water to aquifers, especially on its south side and some processes, which restrict Watarase River seepage flow from the river channel into its north side aquifers probably occur.

3.2. Hydrochemical characteristics

The EC reflects the total dissolved ion concentrations in water bodies, and to a certain extent, the length of flow paths and residence times underground (Song et al., 2006). The EC values of groundwater ranged from 11.9 to 44.4 mS/m, while those of river water ranged from 8.3 to 18.1 mS/m (Table 1). The lowest EC for groundwater was found at AW11, which was a very shallow well situated in the foothills, suggesting a shallow flow path along the hillslope with a relatively short residence time. The highest EC for groundwater was found at AW7, where the d-excess value was lowest, indicating an evaporative enrichment effect. The second highest EC of 36.6 mS/m was found at AW9, indicating the relatively longer residence time for the groundwater at this site.

The groundwater pH ranged from 6.11 to 7.53, with the highest value being observed at the deepest well (AW6, 150 m). The depths of the other private wells and some municipal wells (AT1, AT2, AT3, and AT5) were less than 12 m, while that of AW9 is unknown. Lower pH values (e.g., < 6.0) were found in very shallow wells in the foothills (AW 11).

The trilinear diagram suggests that $Ca\text{-}HCO_3$ is the dominant hydrochemical facies in the study area (Fig. 7), which is common to ordinary groundwater systems. However, for AW9 and AW6, the proportion of Ca^{2+} relative to the total cations (in meq/L) is lower and that of Na^{+} is higher than for the other wells. These characteristics are similar to those for tributaries of the Watarase River and may reflect geology specific to their recharge areas. Groundwater in the foothills (AW9, AW11 and AW12) and from a deep well (AW6), as well as water from the tributaries (AR2, AR3 and AR4) was characterized by poor SO_4^{2-} content. Conversely, water samples from the Watarase

River and the adjacent groundwater had relatively high SO_4^{2-} contents. Because the absolute SO_4^{2-} concentration was greater in groundwater than in water from the Watarase River, the SO_4^{2-} likely originated from sediments deposited by the river rather than the river water itself.

NO_3^- was detected in all river water and groundwater samples except for AW7 and AW9. These findings suggest a certain measure of contamination by fertilizers, sewage and acid deposition. The absence of NO_3^- indicates that the water has never been contaminated or that natural attenuation of nitrate (i.e., denitrification) has occurred in the system.

3.3 End-member mixing analysis

End-member mixing analysis (EMMA) based on the mass balance of tracers has conventionally been used for hydrograph separation (Burns et al., 2001; Doctor et al., 2006). EMMA can also be used to evaluate the contribution ratio of each recharge source of groundwater (Wakui and Yamanaka, 2006; Nakaya et al., 2007; Qin et al., 2011). This technique assumes the following (Barthold et al., 2011): (1) groundwater is a mixture of source substances with a fixed composition; (2) the mixing process is linear and completely dependent on hydrodynamic mixing; (3) the substances used as tracers are conservative; and (4) the source substances have extreme concentrations.

Previous studies have shown that oxygen and hydrogen stable isotope compositions of water have the potential for use in tracing both sources and flow paths in groundwater systems (Nakaya et al., 2007). Chloride is a very conservative tracer, and Subyani (2004) demonstrated its usefulness as a groundwater tracer to evaluate groundwater recharge in alluvial sediments.

Fig. 8 shows a plot of annual (arithmetic) mean δ values against Cl^- in river water and groundwater. Data for all groundwater samples except AW7 are plotted within a triangle. Watarase River water is clearly the end-member corresponding to the lower left vertex of the triangle. Local precipitation had estimated long-term mean δ values and low chloride concentrations and was therefore likely the end-member forming the upper left vertex. Because the chloride concentration of precipitation is not highly variable in space, the chloride concentration of 0.5 mg/L for precipitation at a nearby city (Miyoshi, 2012; personal communication) was used. The δ values and Cl^- concentration of this end-member were similar to those of samples collected from the tributaries (except AR4). The third end-member appears to have moderate δ values and a high Cl^- concentration, which is similar to AW9. As mentioned above, the hydrochemical characteristics of groundwater at AW9 suggest a deep, long flow path. Therefore, this end-member is considered to be the mountain block recharge component. The medium δ values of this end-member indicate that mountain block groundwater was recharged at an elevation between those of the upper Watarase River watershed and the present study area. The reasons for the high Cl^- in the mountain block groundwater are discussed later.

It should be noted that the AW7 groundwater and AR4 river water differed from the other samples. The isotopic signatures of groundwater at AW7 suggest evaporative enrichment with kinetic fractionation (Section 3.1). However, the high Cl^- concentration of this sample cannot be explained solely by such enrichment, indicating mixing with high Cl^- water. According to Miyazaki et al. (2005), the Cl^- concentration of paddy field water ranged from 0.15 to 1.46 mmol/L (5.3 to 51.7 mg/L) at an area adjacent to the present study area. Moreover, the d-excess of paddy field water is generally low because of direct evaporation from water surfaces (Wakui and Yamanaka, 2006). Thus, it is likely that groundwater at AW7 is affected by paddy field water. Indeed, paddy fields comprise one of the dominant land uses in areas north of AW7. Anaerobic environments below paddy fields may have enhanced denitrification. Although river water at AR4 had similar characteristics, its d-excess was not very low. Therefore, this water may be affected by sewage rather than paddy field water. Consequently, data for AW7 are not suitable for EMMA.

Except for AW7, the groundwater δ values and Cl^- concentrations can be used for EMMA assuming three end-members: Watarase River water, local precipitation and mountain block groundwater. The contribution ratio (*R*) from each of the potential sources was estimated using the following equations:

$$R_r = \frac{(\delta_g - \delta_m)(c_p - c_m) - (c_g - c_m)(\delta_p - \delta_m)}{(\delta_r - \delta_m)(c_p - c_m) - (c_r - c_m)(\delta_p - \delta_m)} \quad (1)$$

$$R_p = \frac{(\delta_g - \delta_m)(c_r - c_m) - (c_g - c_m)(\delta_r - \delta_m)}{(\delta_p - \delta_m)(c_r - c_m) - (c_p - c_m)(\delta_r - \delta_m)} \quad (2)$$

$$R_m = 1 - R_r - R_p \quad (3)$$

where δ is the $\delta^{18}O$ or δD; c is the Cl^- concentration; and g, r, p and m denote groundwater at each location, Watarase River water, local precipitation and mountain block groundwater, respectively. Although δ_m and c_m cannot be determined exactly, those for groundwater at AW9 were used as approximations. If the plots of groundwater fall outside of the three end-member model, the contribution ratio for the outliers can be estimated by the method described by Liu et al. (2004). Both $\delta^{18}O$ vs. Cl and δD vs. Cl were applied.

Considering the uncertain composition/concentration of end-members and the resultant mixtures (i.e., groundwater samples), the standard error of the estimated contribution ratio was computed by error propagation analysis (Phillips and Gregg, 2001). The standard deviation of the δ values and Cl^- concentration of groundwater (including AW9 as mountain block recharge) and Watarase River water were used as a measure of the uncertainty. The potential error of long-term mean δ values of local precipitation, which may be due to seasonal and inter-annual variations, was estimated based on the standard deviation of δ values for all river water samples. The uncertainty in Cl^- concentration for local precipitation and some groundwater samples were assumed to be 0.5 mg/L, which is the mean standard deviation of Cl^- concentrations of known groundwater samples.

The estimated contribution ratios and their possible errors are shown in Fig. 9. The errors ranged from 3 to 10% for all wells except AW11. The difference in estimated ratios between $\delta^{18}O$ and δD ranged from 0 to 13%. Taken together, these findings suggest that the results of EMMA are considerably reliable, with a 10% error range. Although river seepage contribution ratio of 16% is found at AW11, which is located far from the river, the potential error of ±17% at this well is relatively large. As mentioned above, the hydrochemical characteristics of groundwater at AW11 indicate its shallow flow path and relatively short residence time. Therefore, the observed δ values of the water should be affected by the lower δ_p in the study period rather than the long-term mean values used for the EMMA. Thus, this error can be attributed to the difference in the time scale deterring δ_p, and the contribution of the Watarase river water at AW11 should be nonexistent.

Even with the errors in the estimated contribution ratios (Fig. 9), the general characteristics of their spatial distribution patterns (Fig. 10) do not change very much, indicating that the results obtained are fairly insensitive to errors. These findings suggest that the contribution ratio from the Watarase River water was extremely high (up to 94%) at wells adjacent to the river channel. However, the distribution of contribution ratios of river seepage was asymmetric with respect to the Watarase River channel. As shown in Figure 11, the contribution of river seepage decreased with increasing distance from the river on both the south and north sides. The river recharged systems as far as 5 km to the south (i.e., plain side) and 1.6 km to the north (i.e., mountain side). The steeper slope of the ground near the mountain is expected to produce faster groundwater flow from the mountain to the river and thus reduce groundwater flow from the river to the north. Thus, the distance can be considered an important factor controlling the contribution ratio of the river water to the groundwater, while the relationship between these factors is modified by topographic conditions such as slope.

Direct infiltration of local precipitation is greatest in the foothills (AW11 and AW12) and areas far from the Watarase River in the plain (AW5). Even at areas along the Watarase River (AT5, AT7 and AW8), the contribution ratio of direct infiltration is ≥50%. The absolute value of the recharge rate by local precipitation should not differ greatly among locations; therefore, reducing the local precipitation contribution will indicate the additional recharge by the river and/or mountain block groundwater. The spatial distribution pattern of the contribution ratios obtained from EMMA indicates where such additional recharge occurs and how the recharge waters flow.

The contribution of the mountain block groundwater to aquifers (mountain block recharge) was remarkably high at the central portion of the study area north of the Watarase River (AW9, AW8 and AT5). In contrast, the contribution of the river water at AW8 and AT5 was nonexistent or negligible, despite the proximity to the river. The AW9, AW8 and AT5 were situated around the estimated axis of the syncline and had layers of chert and sandstone (Fig. 2), which suggests that the syncline structure promoted the mountain block recharge at a particular area around the wells while hindering the flow of water from the river channel to the mountain side. These results agree with those of Laronne Ben-Itzhak and Gvirtzman (2005), who found that groundwater could flow from mountain aquifers to rift valley aquifers along synclinal axes. The high Cl^- concentration observed at AW9 may reflect dissolution of the rocks or solute enrichment by transpiration (not evaporation), which does not induce isotopic fractionation. Since the Na^+, Mg^{2+} and HCO_3^- concentrations were also high at AW9, dissolution of the rocks may be a major cause of high Cl^-. Although this appears to violate the third assumption of the model, the EMMA results are still valid for tracing the mixing of groundwater in the plain aquifer since such sediment is less easily dissolved.

As mentioned above, the major factors controlling the contribution ratio of the river water at each well are the distance from the river, slope, and hydrogeological conditions such as syncline structure. The groundwater pumping rate at each well may be another potential factor influencing the groundwater recharge and flow system (Kelly, 2002; Yamanaka et al., 2011b). Although Fig. 12 suggests a positive correlation between pumping rate and the river water contribution ratio for some municipal wells (AT3, AT4, AT6 and AT7), the higher contribution ratios are a reflection of the shorter distance from the river (Fig. 11) rather than the sole effect of the pumping rate. Although groundwater pumping may enhance the absolute rates of total recharge, EMMA did not provide strong evidence of its effect on river channel seepage.

Based on the above results, the main recharge source for municipal wells (except AT5) is the Watarase River. The contribution ratios of river water generally exceed 50%.

The greatest contribution ratio for municipal wells was 94%, which was observed at the well with the largest pumping rate (AT3 in Fig. 12). Therefore, the domestic water supply system in this area depends strongly on the quantity and quality conditions of the Watarase River. For example, if upstream river water is regulated by dams or contaminated by accidents, water from municipal wells may be affected, while hydraulic drawdown due to pumping at the wells can be mitigated by river seepage. Conversely, even though AT5 is located very close to the river channel and has high pumping rate, the contribution of Watarase River water to this aquifer is suppressed by mountain block recharge. Thus, this well is not strongly influenced by Watarase River conditions. Furthermore, at direct-recharge-dominated sites, shallow groundwater should be more sensitive to artificial alteration of land use and cover. These findings should be helpful for integrated management of groundwater and surface water resources.

4. Conclusions

Isotope and hydrochemistry analysis indicated that direct infiltration by precipitation, Watarase River seepage and mountain block recharge are the three main recharge sources in the study area. The isotopic signatures revealed an obvious altitude effect, as well as mean residence times of river water and groundwater > 1 year.

EMMA using stable isotope and chloride tracers was shown to be useful for estimation of the contribution ratio of different recharge sources with sufficiently low error (≤ 10%). The results demonstrated that the Watarase River contributes a great amount of water to aquifers along its channel, with the contribution ratio reaching as high as 94%. However, the spatial extent of river-recharged water differs, with the water influencing aquifers for 5 km from the channel and 1.6 km on the plain side and mountain side, respectively. Mountain block recharge is one of the dominant components in a limited area in the foothills. A syncline structure was found to play an important role in transmitting mountain block recharge, and mountain block recharge was shown to suppress river channel seepage into the mountain side aquifers. The distance from the river channel, topography and hydrogeological settings such as syncline were identified as the three major factors controlling the river water contribution ratio.

The major findings of this study will help improve the understanding of recharge processes and dynamics and facilitate integrated management of surface and subsurface water resources. This paper highlights the spatial structure of the groundwater-river interactions and the influence of syncline structure settings on mountain block recharge. To further increase the reliability of EMMA results, combined use of the other approaches such as numerical simulation is necessary.

Acknowledgements

The research was supported in part by the special study fund of Terrestrial Environment Research Center, University of Tsukuba. We wish to thank Masayoshi Yamaguchi, Tadao Matsuzaki and Takashi Arai of the Municipal Water Department, Ashikaga City, for their help in collecting water samples from municipal wells.

References

Aishlin, P., McNamara, J.P., 2011. Bedrock infiltration and mountain block recharge accounting using chloride mass balance. Hydrological Processes, 25(12): 1934-1948.

Barthold, F.K., Tyralla, C., Schneider, K., Vaché, K.B., Frede, H., Breuer, L., 2011. How many tracers do we need for end member mixing analysis (EMMA)? A sensitivity analysis. Water Resources Research, 47, W08519, doi:10.1029/2011WR010604.

Burns, D.A., McDonnell, J.J., Hooper R.P., Peters N.E., Freer, J.E., Kendall, C., Beven K., 2001. Quantifying contributions to storm runoff through end-member mixing analysis and hydrologic measurements at the Panola Mountain Research Watershed (Georgia, USA). Hydrological Processes, 15(10): 1903-1924.

Clark, I., Fritz, P., 1997. Environmental Isotopes in Hydrogeology. CRC Press, New York, 328pp.

Craig, H., 1961. Isotopic Variations in Meteoric Waters. Science, 133(346): 1702-1703.

Dansgaard, W., 1964. Stable Isotopes in Precipitation. Tellus, 16(4): 436-468.

de Vries, J.J., Simmers, I., 2002. Groundwater recharge: an overview of processes and challenges. Hydrogeology Journal, 10(1): 5-17.

Doctor, D.H., Alexander Jr, E.C., Petrič, M., Kogovšek, J., Urbanc, J., Lojen, S., Stichler, W., 2006. Quantification of karst aquifer discharge components during storm events through end-member mixing analysis using natural chemistry and stable isotopes as tracers. Hydrogeology Journal, 14(7): 1171-1191.

Gupta, P., Noone, D., Galewsky, J., Sweeney, C., Vaughn, B.H., 2009. Demonstration of high-precision continuous measurements of water vapor isotopologues in laboratory and remote field deployments using wavelength-scanned cavity ring-down spectroscopy (WS-CRDS) technology. Rapid Communications in Mass Spectrometry, 23(16): 2534-2542.

Kalbus, E., Reinstorf, F., Schirmer, M., 2006. Measuring methods for groundwater - surface water interactions: a review. Hydrology and Earth System Sciences, 10(6): 873-887.

Kelly, P.B., 2002. Ground-water flow simulation and chemical and isotopic mixing equation analysis to determine source contributions to the Missouri River alluvial aquifer in the vicinity of the independence, Missouri, well field. U.S. Geological Survey Water-Resources Investigations Report, 2002-4208, 31 pp.

Lambs, L., 2004. Interactions between groundwater and surface water at river banks and the confluence of rivers. Journal of Hydrology, 288(3-4): 312-326.

Laronne Ben-Itzhak, L., Gvirtzman, H., 2005. Groundwater flow along and across structural folding: an example from the Judean Desert, Israel. Journal of Hydrology, 312(1-4): 51-69.

Liu, F.J., Williams, M.W., Caine, N., 2004. Source waters and flow paths in an alpine catchment, Colorado Front Range, United States. Water Resources Research, 40(9), W09401, doi:10.1029/2004WR003076.

Manning, A.H., Solomon, D.K., 2005. An integrated environmental tracer approach to characterizing groundwater circulation in a mountain block. Water Resources Research, 41(12), W12412, doi:10.1029/2005WR004178.

Mikita, M., Yamanaka, T., Lorphensri, O., 2011. Anthropogenic changes in a confined groundwater flow system in the Bangkok basin, Thailand, part I: was groundwater-recharge enhanced?. Hydrological Processes, 25(17): 2726-2733.

Miyazaki, N., Namewada, K., Iwasaki, S., 2005. Quality changes of agricultural water passing through paddy fields. Bulletin of the Tochigi Prefectural Agricultural Experiment Station, 55: 45-55 (*in Japanese with English abstract*).

Nakaya, S., Uesugi, K., Motodate, Y., Ohmiya, I., Komiya, H., Masuda, H., Kusakabe, M., 2007. Spatial separation of groundwater flow paths from a multi-flow system by a simple mixing model using stable isotopes of oxygen and hydrogen as natural tracers. Water Resources Research, 43(9), W09404, doi:10.1029/2006WR005059.

Phillips, D.L., Gregg, J.W., 2001. Uncertainty in source partitioning using stable isotopes. Oecologia, 127(2): 171-179.

Poage, M.A., Chamberlain, C.P., 2001. Empirical relationships between elevation and the stable isotope composition of precipitation and surface waters: Considerations for studies of paleoelevation change. American Journal of Science, 301: 1-15.

Qin, D., Qian, Y., Han, L., Wang, Z., Li, C., Zhao, Z., 2011. Assessing impact of irrigation water on groundwater recharge and quality in arid environment using CFCs, tritium and stable isotopes, in the Zhangye Basin, Northwest China. Journal of Hydrology, 405(1-2): 194-208.

Sanz, D., Castano, S., Cassiraga, E., Sahuquillo, A., Gomez-Alday, J. J., Pena, S., Calera, A., 2011. Modeling aquifer-river interactions under the influence of groundwater abstraction in the Mancha Oriental System (SE Spain). Hydrogeology Journal, 19(2): 475-487.

Scanlon, B.R., Healy, R.W., Cook, P.G., 2002. Choosing appropriate techniques for quantifying groundwater recharge. Hydrogeology Journal, 10(1): 18-39.

Song, X., Liu, X., Xia, J., Yu, J., Tang, C., 2006. A study of interaction between surface water and groundwater using environmental isotope in Huaisha River basin. Science in China Series D: Earth Sciences, 49(12): 1299-1310.

Subyani, A.M., 2004. Use of chloride-mass balance and environmental isotopes for evaluation of groundwater recharge in the alluvial aquifer, Wadi Tharad, western Saudi Arabia. Environmental Geology, 46(6-7): 741-749.

Vanderzalm, J.L. et al., 2011. Recharge sources and hydrogeochemical evolution of groundwater in alluvial basins in arid central Australia. Journal of Hydrology, 397(1-2): 71-82.

Wakui, H., Yamanaka, T., 2006. Sources of groundwater recharge and their local differences in the central part of Nasu fan as revealed by stable isotope. Groundwater Hydrology, 48(2): 263-277 (*in Japanese with English abstract*).

Waseda, A., Nakai, N., 1983. Isotopic compositions of meteoric and surface waters in central and northeast Japan. Chikyukagaku, 17: 83-91 (*in Japanese*).

Wilson, J.L., Guan, H., 2004. Mountain-block hydrology and mountain-front recharge, in: Phillips, F.M., Hogan, J., Scanlon, S., (Eds.), Groundwater Recharge in a Desert Environment: the Southwestern United States, Water Science and Application Series, vol. 9. American Geophysical Union, Washington, D.C, pp. 113-137.

Xi, H., Feng, Q., Si, J., Chang, Z., Cao, S., 2010. Impacts of river recharge on groundwater level and hydrochemistry in the lower reaches of Heihe River Watershed, northwestern China. Hydrogeology Journal, 18(3): 791-801.

Yamanaka, T., Mikita, M., Lorphensri, O., Shimada, J., Kagabu, M., Ikawa, R., Toshio, N., Tsujimura, M., 2011a. Anthropogenic changes in a confined groundwater flow system in the Bangkok Basin, Thailand, part II: how much water has been renewed? Hydrological Processes, 25(17): 2734-2741.

Yamanaka, T., Onda, Y., 2011. On measurement accuracy of liquid water isotope analyzer based on wavelength-scanned cavity ring-down spectroscopy (WS-CRDS). Bulletin of Terrestrial Environmental Research Center, University of Tsukuba, 12: 31-40 (*in Japanese*).

Yamanaka, T., Shimada, J., Tsujimura, M., Lorphensri, O., Mikita, M., Hagihara, A., Onodera, S., 2011b. Tracing a confined groundwater flow system under the pressure of excessive groundwater use in the lower central plain, Thailand. Hydrological Processes, 25(17): 2654-2664.

Yuan, R., Song, X., Zhang, Y., Han, D., Wang, S., Tang, C., 2011. Using major ions and stable isotopes to characterize recharge regime of a fault-influenced aquifer in Beiyishui River Watershed, North China Plain. Journal of Hydrology, 405(3-4): 512-521.

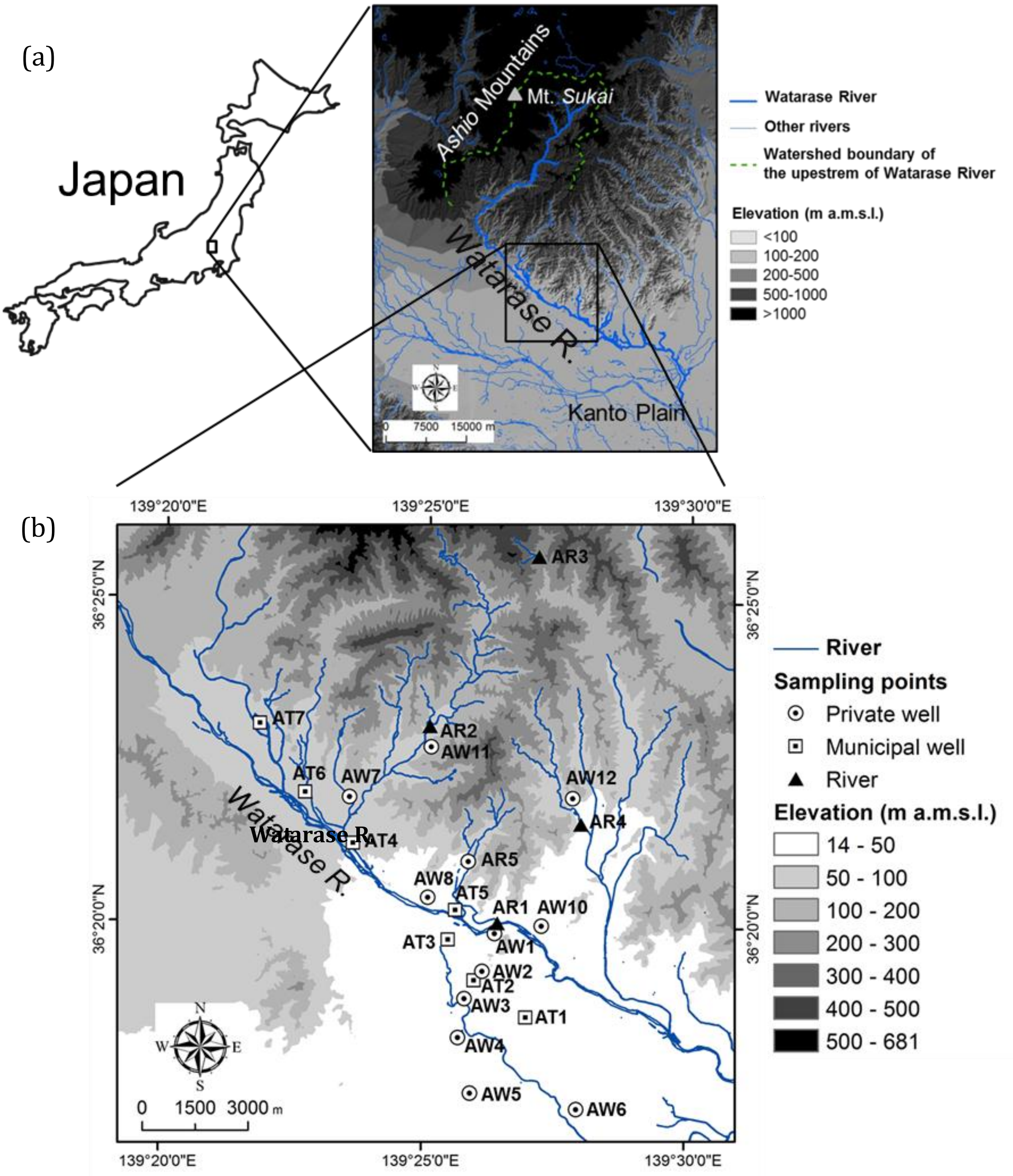

Fig. 1. Maps of (a) the headstream and watershed of the Watarase River, and (b) the study area and sampling points.

(a)

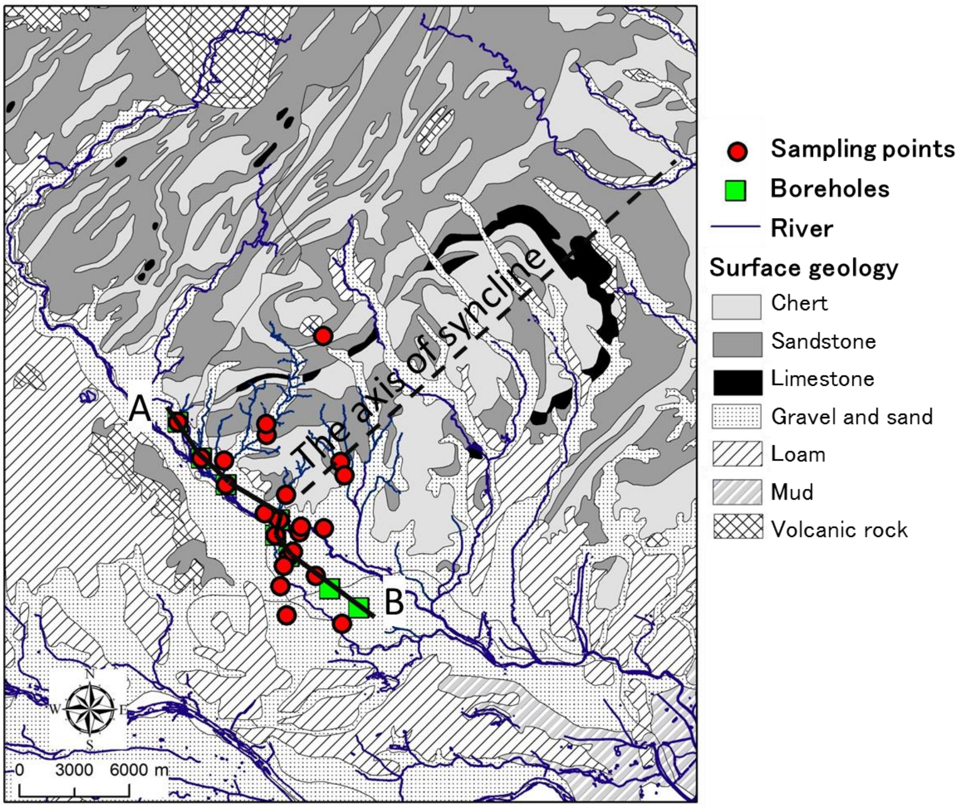

(b)

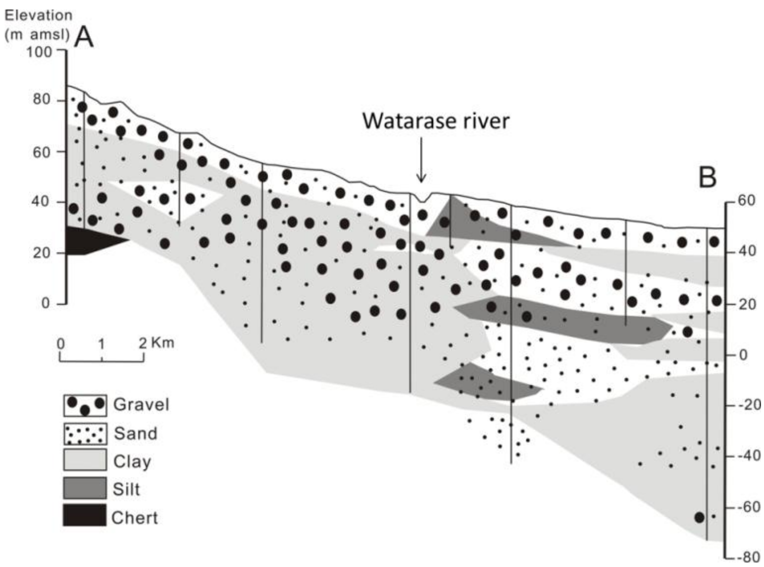

Fig. 2. Surficial geology map (a) of the study area (National Land Survey Division, Land and Water Bureau, Japan; http://tochi.mlit.go.jp/tockok/) with (b) cross-section A-B showing lithology of aquifers (drawn based on borehole logs).

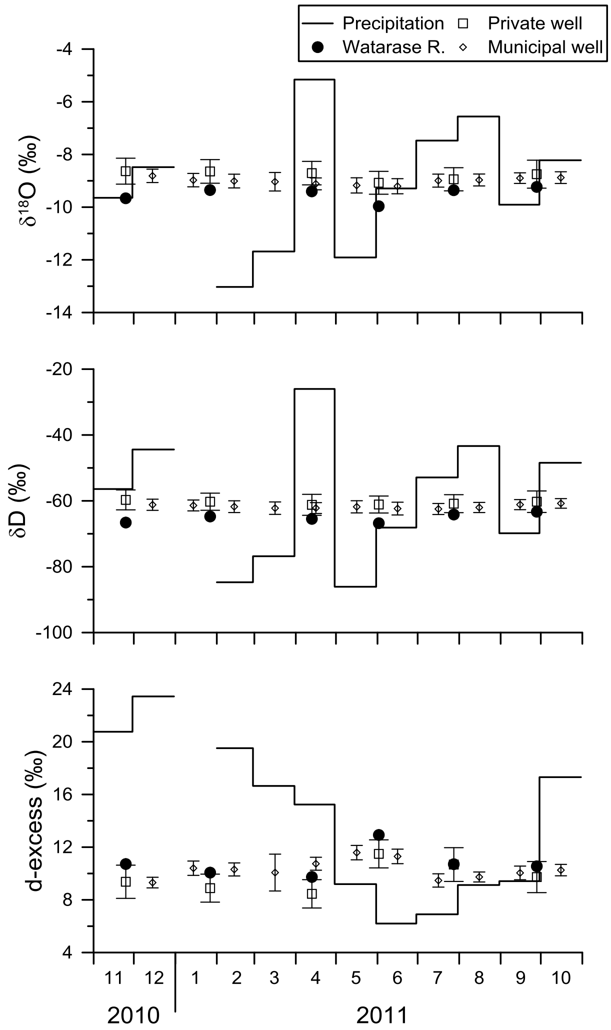

Fig. 3. Temporal variations of $\delta^{18}O$, δD and d-excess in precipitation, Watarase river water and groundwater during the study period.

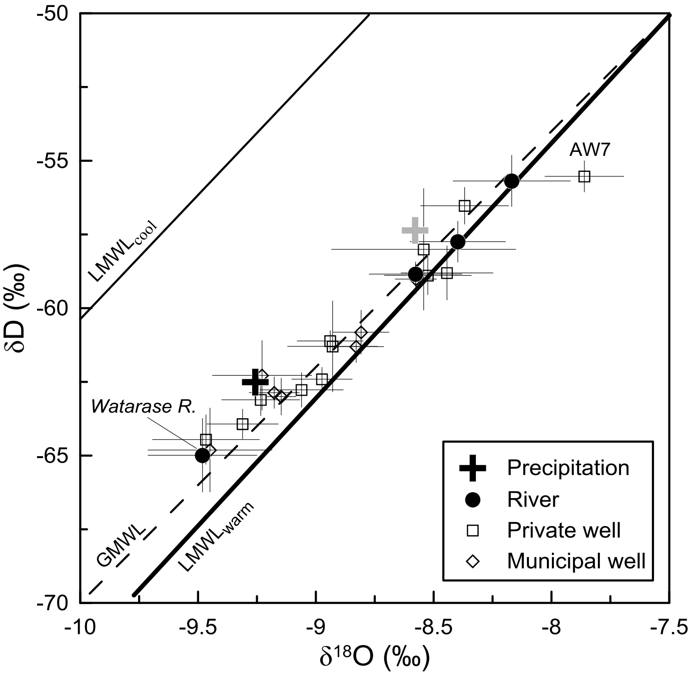

Fig. 4. Plot of $\delta^{18}O$ vs. δD of river and groundwater samples. The global meteoric water line and local meteoric water lines (in cool season and warm season) are added. Black cross is weighted (by monthly precipitation amount) mean precipitation and gray cross represent mean precipitation weighted by long-term mean precipitation amount.

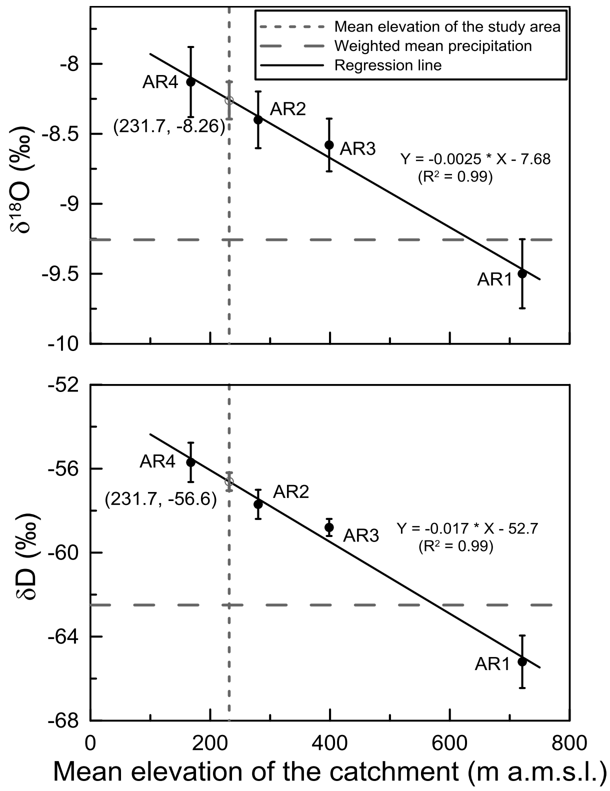

Fig. 5. Mean $\delta^{18}O$ and δD of river water vs. mean elevation of the catchment. The gray open circles represent estimated long-term mean δ values of precipitation corresponding to the mean elevation of the study area and the gray error bars are estimated standard deviation for long-term mean δ values of precipitation.

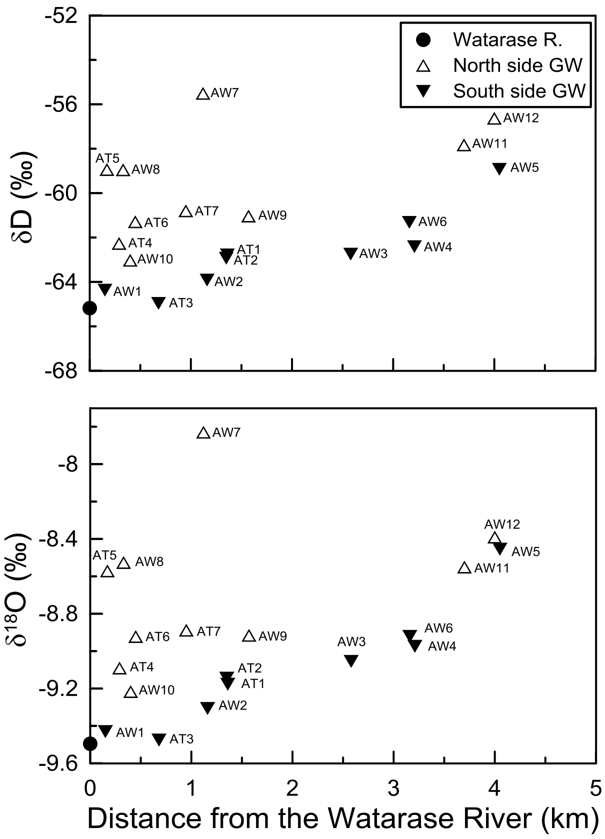

Fig. 6. Annual mean $\delta^{18}O$ and δD of groundwater and their relationship with distance from the Watarase River. The annual mean $\delta^{18}O$ and δD of Watarase River water was also plotted for reference.

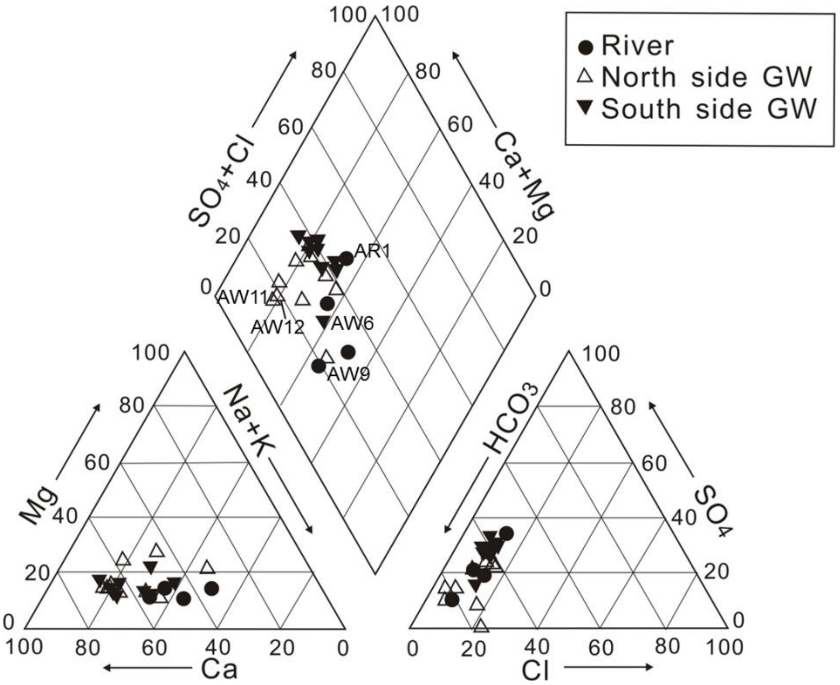

Fig. 7. Piper diagram of groundwater and river water samples in the study area.

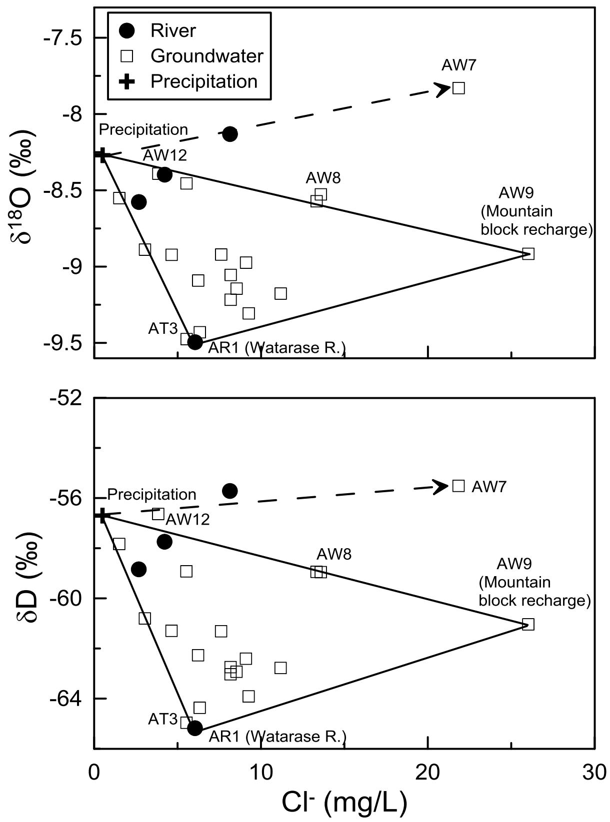

Fig. 8. Relationship of arithmetic mean annual $\delta^{18}O$, δD and Cl^- concentration in river water and groundwater.

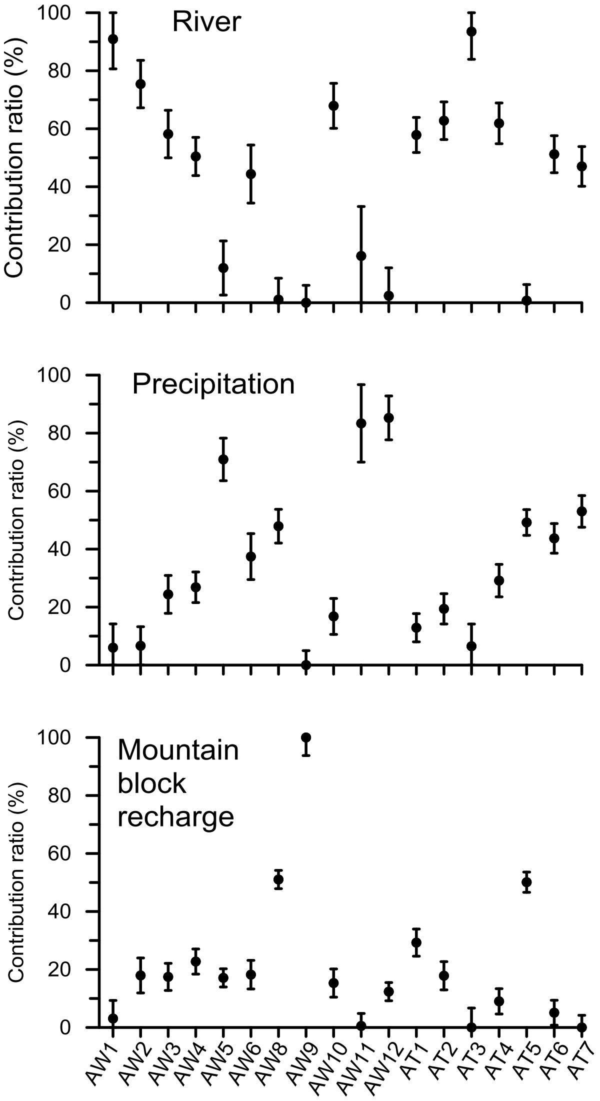

Fig. 9 The contribution ratios and corresponding estimation errors of recharge sources for wells.

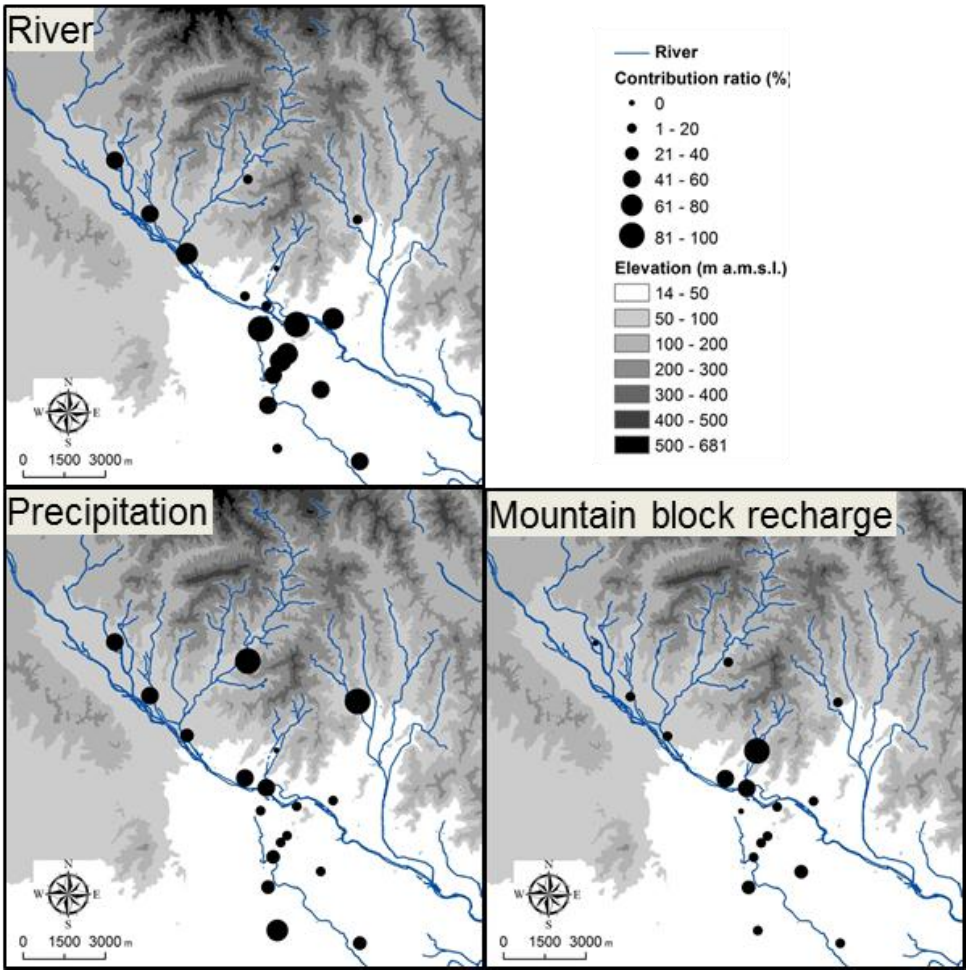

Fig. 10. Spatial distribution of contribution ratios of groundwater recharge sources.

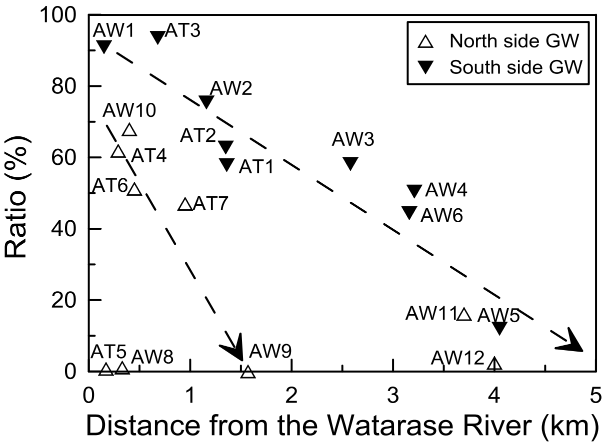

Fig. 11. Relationship of river water contribution ratio and distance from the Watarase River.

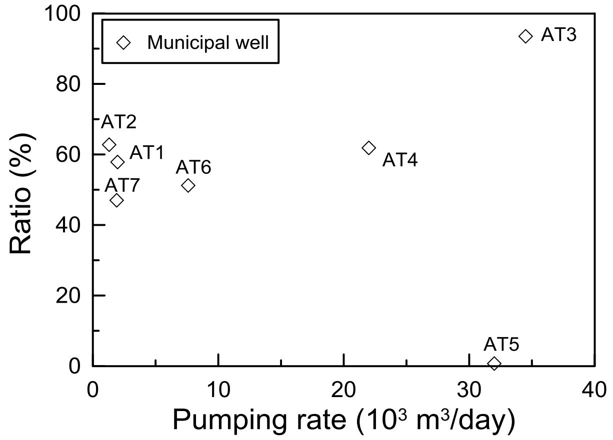

Fig. 12. Relationship of river water contribution ratio and pumping rate.

Table 1 The analyzed hydrochemical and isotopic items of groundwater and river samples

	Hydrochemistry										Isotope	
ID	EC ms/m	pH	Na^+ mg/L	K^+ mg/L	Ca^{2+} mg/L	Mg^{2+} mg/L	Cl^- mg/L	SO_4^{2-} mg/L	HCO_3^- mg/L	NO_3^- mg/L	$\delta^{18}O$ ‰	δD ‰
AW1	17.1	6.40	13.5	1.6	20.1	2.9	6.3	23.7	55.5	9.3	-9.43	-64.4
AW2	22.8	6.52	20.1	2.1	32.3	4.9	9.3	29.4	71.1	13.4	-9.31	-63.9
AW3	29.4	6.62	16.4	2.3	42.2	6.8	8.2	45.7	101.5	14.6	-9.05	-62.7
AW4	27.3	6.51	24.0	2.9	37.1	10.4	9.1	36.7	101.2	2.7	-8.97	-62.4
AW5	19.9	6.29	11.5	2.8	32.5	3.9	5.5	28.4	76.9	3.3	-8.45	-58.9
AW6	16.8	7.53	17.5	1.5	18.5	4.4	7.6	13.1	73.6	4.7	-8.92	-61.3
AW7	44.4	6.73	23.9	1.7	34.5	13.5	21.8	18.1	168.9	0.0	-7.83	-55.5
AW8	26.0	6.35	20.4	1.9	32.7	5.2	13.6	27.9	94.7	13.9	-8.53	-59.0
AW9	36.6	6.66	43.9	2.3	27.2	11.7	26.0	2.8	156.7	0.0	-8.92	-61.0
AW10	21.2	6.36	19.7	2.7	25.2	3.4	8.2	25.5	74.2	10.8	-9.22	-63.0
AW11	11.9	6.11	5.9	0.9	18.3	2.6	1.5	8.9	57.6	6.9	-8.55	-57.8
AW12	15.3	6.46	8.6	2.6	23.9	6.6	3.8	10.2	94.7	9.6	-8.39	-56.6
AT1			11.4	2.1	34.6	4.9	11.2	33.3	98.7	16.7	-9.18	-62.8
AT2			8.3	1.6	33.4	5.3	8.5	37.3	106.7	15.3	-9.14	-62.9
AT3			9.6	2.3	24.3	2.8	5.5	18.0	48.4	7.6	-9.48	-65.0
AT4			9.3	1.6	23.9	3.3	6.2	18.5	58.2	8.3	-9.09	-62.3
AT5			15.3	2.5	44.5	6.8	13.3	33.7	107.9	14.3	-8.57	-58.9
AT6			7.1	1.7	23.1	3.4	4.6	15.9	61.9	9.9	-8.92	-61.3
AT7			7.0	1.5	25.3	3.6	3.0	10.2	63.8	5.5	-8.89	-60.8
AR1	12.6	7.37	15.6	1.7	22.3	2.6	6.0	19.5	38.6	6.0	-9.50	-65.2
AR2	10.6	6.86	18.9	1.0	11.3	2.5	4.2	10.5	47.2	4.8	-8.40	-57.7
AR3	8.3	7.10	12.5	0.8	11.2	1.4	2.7	3.8	41.4	7.8	-8.58	-58.8
AR4	18.1	7.19	16.8	2.1	20.0	3.3	8.1	14.3	65.6	7.3	-8.13	-55.7